JACC: BASIC TO TRANSLATIONAL SCIENCE VOL. 7, NO. 9, 2022

ORIGINAL RESEARCH - PRECLINICAL

Therapeutics That Promote Sympathetic Reinnervation Modulate the Inflammatory Response After Myocardial Infarction

Joseph J. Sepe, PhD,[a,b] Ryan T. Gardner, PhD,[a,b] Matthew R. Blake, BS,[a] Deja M. Brooks, BS,[a] Melanie A. Staffenson, BS,[a] Courtney B. Betts, PhD,[c,d] Sam Sivagnanam, MS,[c,d] William Larson, BS,[c,d] Sushil Kumar, PhD,[c,d] Richard G. Bayles, PhD,[a] Haihong Jin, PhD,[a] Michael S. Cohen, PhD,[a] Lisa M. Coussens, PhD,[c,d] Beth A. Habecker, PhD[a,b]

VISUAL ABSTRACT

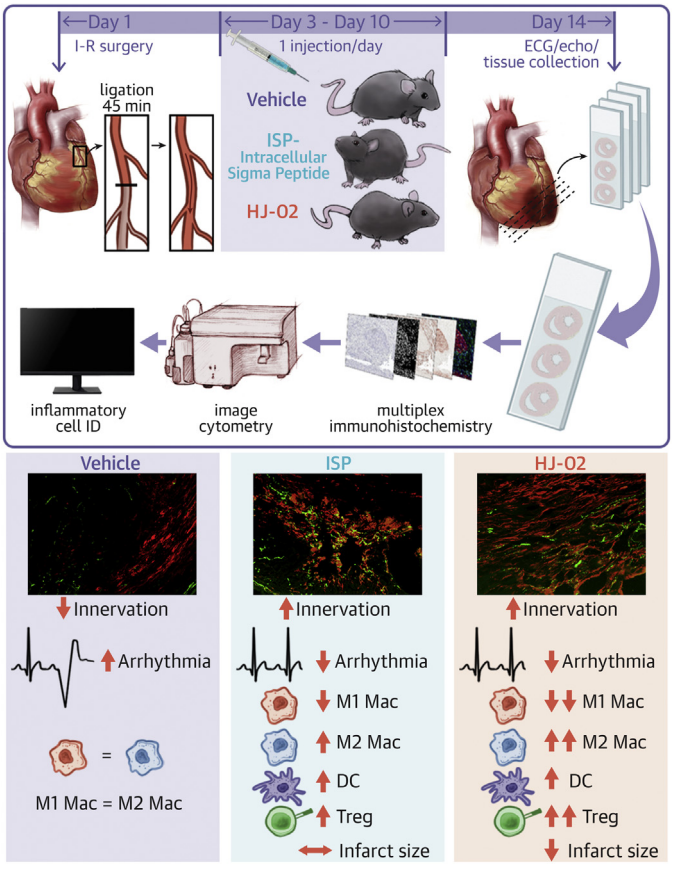

Sepe JJ, et al. J Am Coll Cardiol Basic Trans Science. 2022;7(9):915–930.

HIGHLIGHTS

- **Quantitative multiplex immunohistochemistry employing 23 antibodies was used to identify the immune cells present in the left ventricle 2 weeks after ischemia-reperfusion.**
- **Two therapeutics (ISP and HJ-02), administered on days 3-10 after ischemia-reperfusion, restored sympathetic innervation throughout the left ventricle and decreased arrhythmia susceptibility.**
- **Treatment with ISP and HJ-02 shifted the immune response from inflammatory to reparative, with fewer pro-inflammatory (M1-like) macrophages and increased numbers of regulatory T cells and reparative (M2-like) macrophages in reinnervated hearts.**
- **HJ-02 stimulated a significantly greater shift from pro-inflammatory to reparative cell types compared with ISP, which coincided with decreased infarct size and normal cardiac output and ejection fraction.**
- **Neither ISP nor HJ-02 altered macrophage phenotypes in cultured peritoneal macrophages, which suggested that reinnervation contributes to the M1 to M2 shift in vivo.**

From the [a]Department of Chemical Physiology and Biochemistry, Oregon Health and Science University, Portland, Oregon, USA; [b]Department of Medicine, Knight Cardiovascular Institute, Oregon Health and Science University, Portland, Oregon, USA; [c]Department of Cell, Developmental and Cancer Biology, Oregon Health and Science University, Portland, Oregon, USA; and the [d]Knight Cancer Institute, Oregon Health and Science University, Portland, Oregon, USA.

ISSN 2452-302X https://doi.org/10.1016/j.jacbts.2022.04.009

JACC: BASIC TO TRANSLATIONAL SCIENCE VOL. 7, NO. 9, 2022
SEPTEMBER 2022:915–930

ABBREVIATIONS AND ACRONYMS

ACh = acetylcholine

β1-AR = adrenergic receptor

IP = intraperitoneal

ISP = intracellular sigma peptide

MI = myocardial infarction

mIHC = multiplex immunohistochemistry

NE = norepinephrine

PBS = phosphate-buffered saline

Tregs = regulatory T cells

TH = tyrosine hydroxylase

VEH = vehicle

SUMMARY

Myocardial infarction (MI) triggers an inflammatory response that transitions from pro-inflammatory to reparative over time. Restoring sympathetic nerves in the heart after MI prevents arrhythmias. This study investigated if reinnervation altered the immune response after MI. This study used quantitative multiplex immunohistochemistry to identify the immune cells present in the heart 2 weeks after ischemia-reperfusion. Two therapeutics stimulated reinnervation, preventing arrhythmias and shifting the immune response from inflammatory to reparative, with fewer pro-inflammatory macrophages and more regulatory T cells and reparative macrophages. Treatments did not alter macrophage phenotype in vitro, which suggested reinnervation contributed to the altered immune response. (J Am Coll Cardiol Basic Trans Science 2022;7:915–930)

Myocardial infarction (MI) triggers a robust inflammatory response that results in recruitment and activation of innate and adaptive immune cells.[1,2] This inflammatory response induces numerous responses that are vital for cardiac repair but can lead to pathological remodeling of the myocardium and eventual cardiac dysfunction. The composition of immune cells present in the heart following ischemia-reperfusion changes over time.[1,3] The initial inflammatory phase is characterized by proteolysis, phagocytosis, and generation of pro-inflammatory cytokines.[4,5] Suppression of inflammation and increased cells with a reparative phenotype, including reparative macrophages[6] and regulatory T cells (Tregs),[7] characterize the second phase of the healing process. In the final phase of recovery, a mature scar is formed.[8]

Myocardial ischemia-reperfusion damages nerves in the heart in addition to cardiomyocyte injury and death.[9,10] Cardiac sympathetic nerves innervate the sinoatrial and atrioventricular nodes, conduction system, atria, and ventricles, where they release norepinephrine (NE) to increase heart rate, conduction velocity, and contractility by activating β1-adrenergic receptors (AR). Ischemia-reperfusion leads to degeneration of nerve fibers in the myocardium, and several clinical trials have concluded that the amount of sympathetic denervation in the heart after MI predicts the probability of serious ventricular arrhythmias.[11-13] We previously showed that chondroitin sulfate proteoglycans in the cardiac scar prevent sympathetic nerves from reinnervating the infarct.[9] These proteoglycans act through protein tyrosine phosphatase receptor−σ on sympathetic neurons to prevent nerve regeneration.[9] Restoring sympathetic innervation throughout the left ventricle after MI by removing or disrupting protein tyrosine phosphatase receptor−σ normalizes NE content, myocyte β-AR signaling, cardiac electrophysiology, and myocyte calcium handling, rendering hearts resistant to isoproterenol-induced arrhythmias.[10]

MI also induces cholinergic transdifferentiation of cardiac sympathetic nerves, which transiently produce acetylcholine (ACh), along with NE, during the first 2 weeks after MI.[14] It is not known if reinnervation of the developing infarct alters the inflammatory response, but noradrenergic sympathetic transmission regulates inflammation in multiple contexts, having both pro- and anti-inflammatory effects.[15,16] Furthermore, cholinergic transmission is anti-inflammatory in the heart.[17] We hypothesized that restoring sympathetic transmission during infarct development would alter the immune cell types present in the scar 2 weeks after ischemia-reperfusion, when sympathetic nerves contain both NE and ACh.

Quantitative multiplex immunohistochemistry (mIHC) enables comprehensive phenotyping of immune cells present in tissues using single formalin-fixed, paraffin-embedded tissue sections.[18,19] In the present study, we used this novel platform in the heart to characterize the immune response following MI. Using a panel of 23 different antibodies to identify leukocyte subsets that reflected both innate and adaptive immune cell lineages present in the heart after MI, we found that treatments promoting

The authors attest they are in compliance with human studies committees and animal welfare regulations of the authors' institutions and Food and Drug Administration guidelines, including patient consent where appropriate. For more information, visit the Author Center.

Manuscript received March 11, 2022; revised manuscript received April 13, 2022, accepted April 15, 2022.

sympathetic reinnervation altered the repertoire of immune cells present. We showed that novel small molecules, which restored sympathetic neuron growth through chondroitin sulfate proteoglycans in vitro,[20] promoted sympathetic regeneration in the heart after MI. Peptide and small molecule therapeutics that stimulated sympathetic reinnervation significantly increased dendritic cells, Treg cells, and reparative (M2-like) macrophages present in the infarcted heart, while suppressing inflammatory (M1-like) macrophages.

METHODS

ANIMALS. C57BL/6J mice were obtained from Jackson Labs. Age- and sex-matched mice 12-18 weeks old were used for all experiments. All mice were kept on a 12:12 hour light-dark cycle with ad libitum access to food and water. All procedures were approved by the OHSU Institutional Animal Care and Use Committee and complied with the Guide for the Care and Use of Laboratory Animals published by the National Academies Press (8th edition).

ISCHEMIA-REPERFUSION SURGERY AND TREATMENTS. Mice underwent left coronary artery ligation to induce myocardial ischemia-reperfusion injury as described previously.[9,21] Briefly, anesthesia was induced with 4% isoflurane and maintained with 2% isoflurane. The left anterior descending coronary artery was ligated for 45 minutes and reperfused by release of the ligature. Mice were given regular food and water until euthanasia and tissue harvest. Meloxicam (5-10 mg/kg subcutaneously) and buprenorphine (0.1 mg/kg) were administered as needed to ensure that animals were comfortable after surgery. All surgical procedures were performed under aseptic conditions. Sham animals underwent the previously described procedure, except for ligation of the left anterior descending coronary artery. Quantitative polymerase chain reaction confirmed induction of infarct-associated genes and suppression of myocyte genes after ischemia-reperfusion[22-24] (Supplemental Figures 1 and 2).

Treatment groups. Mice (4-6 mice/group) were treated once per day on days 3-10 after surgery. Control mice were given intraperitoneal (IP) injections of vehicle (VEH) (5% dimethyl sulfoxide/saline). To promote reinnervation of the left ventricle, mice were treated with either intracellular sigma peptide (ISP) (10 mg/kg IP),[10,25] HJ-01 (10 mg/kg IP), or HJ-02 (10 mg/kg IP).[20]

IN VIVO TELEMETRY. Electrocardiograms were obtained from conscious adult mice using ETA-F10 (Data Sciences International) telemetry implants and analyzed with the Ponemah software (Data Sciences International) as described previously.[10] Devices were implanted at least 5 days before ischemia-reperfusion or sham surgery. Electrocardiographic recordings were obtained 14 days after sham or MI. Premature ventricular complexes were defined as a single premature QRS complex in the absence of a P-wave and were counted for 60 minutes after IP injection of the β-AR agonist isoproterenol (10 μg) to identify isoproterenol-induced arrhythmias. Heart rate was analyzed to confirm that the sinoatrial node response to isoproterenol was similar between groups.

ECHOCARDIOGRAPHY. High-frequency fundamental imaging (Vevo 2100) was performed at 25 to 40 MHz depending on the echocardiographic data that were acquired. Mice were sedated with inhaled isoflurane (1.0%-1.5%). Images were obtained in the parasternal long- and short-axis planes at the mid-papillary level. Measurement of left ventricular end-diastolic and end-systolic areas (short axis) and end-diastolic and end-systolic lengths (long axis) were used to measure left ventricular function. Stroke volume was determined using the product of the left ventricular outflow tract area and the time-velocity integral on pulse-wave Doppler. Cardiac function was analyzed under basal conditions and in response to the β-AR agonist isoproterenol (10 μg or ∼0.5 mg/kg).

INFARCT SIZE. Infarcts were identified 14-15 days after reperfusion using 2 methods in 2 groups of mice: 1) the absence of autofluorescence in frozen sections[26]; and 2) absence of stain in formalin-fixed, paraffin-embedded sections following 1 minute of hematoxylin incubation (Supplemental Figure 3). Five 10-μm sections per heart were photographed and the left ventricular and infarct areas were outlined and quantified using the freehand selection tool in ImageJ. Infarct size was defined as: (infarct area/left ventricular area) × 100. Sections were from the upper, middle, and lower regions of each infarct. Two blinded observers analyzed sections independently, and the results were averaged.

STANDARD IMMUNOHISTOCHEMISTRY. Tissue was collected 14 days after surgery, fixed in 4% paraformaldehyde, frozen, and 10-μm sections generated. Immunohistochemistry for tyrosine hydroxylase (TH) (sympathetic nerves) and fibrinogen (infarct/scar) was carried out as described previously,[9,27] using rabbit anti-TH (1:1000, Millipore Sigma AB152) and Alexa Fluor 488-conjugated rabbit immunoglobulin-G–specific antibody (1:500; Molecular Probes), together with sheep antifibrinogen (1:300, AbD

FIGURE 1 Multiplex Immunohistochemistry (mIHC) Overview

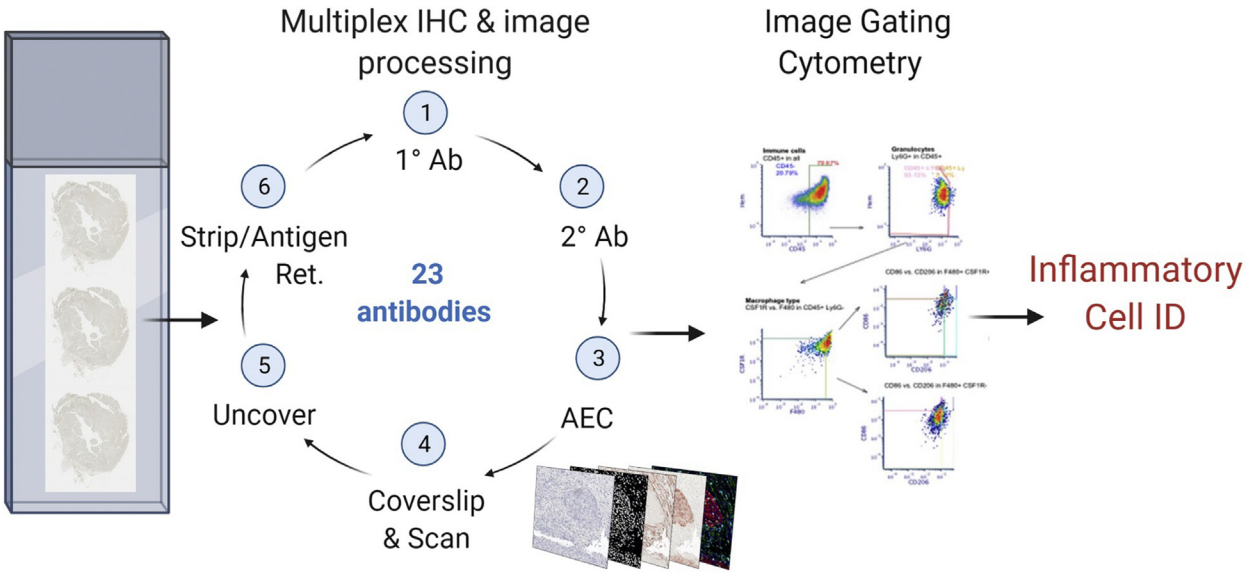

The multiplex immunohistochemistry (mIHC) process begins with multiple cycles of applying specific antibodies of interest to tissue sections, and scanning tissue sections after each stain. After the staining and scanning process, image gating cytometry is used to identify and classify immune cells. Finally, immune cell types are quantified.

Serotec 4440-8004) and Alexa Fluor-568 conjugated sheep immunoglobulin-G–specific antibody (1:500, Molecular Probes). Sections were incubated with sodium borohydride and copper sulfate to decrease autofluorescence. Slides were rinsed 3× 10 minutes with phosphate-buffered saline (PBS), cover slipped, and visualized by fluorescence microscopy. Staining was quantified using the thresholding tool in ImageJ in at least 5 sections per heart. TH+ fiber density was quantified in the infarct and in the area next to the infarct (peri-infarct) as described previously.[27]

mIHC AND IMAGE ACQUISITION. Hearts were excised, rinsed with PBS, fixed for 24 hours in 10% buffered formalin, and dehydrated in 70% ethanol before paraffin embedding and sectioning by the OHSU Histopathology Shared Resource core facility. Four slides, each containing 3 5-μm sections per slide, were processed and used for mIHC from each heart (Figure 1). Sections were deparaffinized, stained with hematoxylin (S3301, Dako), and digitally scanned at 20× magnification on an Aperio AT2 (Leica Biosystems). After the initial hematoxylin stain, sequential IHC was carried out with 23 different antibodies using a method adapted from Banik et al[18] and Tsujikawa et al[19] Each round of IHC included 3 steps before adding the primary antibody: 1) antigen retrieval, boiling for 15 minutes in a pH 6.0 Citra solution (BioGenex); 2) endogenous peroxidase blocking, 20 minutes at room temperature in 0.6% hydrogen peroxide Dako Dual Endogenous Enzyme Block (S2003, Dako); and 3) protein blocking, 10 minutes at room temperature with 5% normal goat serum and 2.5% bovine serum albumin in Tris-buffered saline with 0.1% Tween. Primary antibody was then added, and incubations either occurred for 60 minutes at room temperature, 4 hours at room temperature, or overnight at 4 °C (see Table 1 for details on each antibody). Slides were then washed 3× 2 minutes in TBST, and anti-rat or anti-rabbit Histofine Simple Stain MAX PO horseradish peroxidase–conjugated polymers (Nichirei Biosciences) were added for 30 minutes at room temperature. Slides were again washed 3× 2 minutes in TBST, and antibody was visualized using AEC chromogen (Vector Laboratories). AEC chromogen incubation time was antibody dependent, and antibody-specific incubation times are listed in Table 1. Once the chromogen had developed (visually confirmed by light microscope), slides were digitally scanned at 20× magnification on the Aperio AT2. Sections then underwent a new round of staining, beginning with the stripping and antigen retrieval step described previously. After visualization of all 23 antibodies, a final round of hematoxylin staining was completed,

TABLE 1 Multiplex IHC Antibody Panel and Cell Type Identification: Sequential IHC Antibody Panel Information

Cycle (Round)	Target Antigen	Vendor or Source	Catalog #	Clone	Working Concentration	Duration
	Hematoxylin (initial)					1 min
1 (1)	CSF-1R	Santa Cruz	Sc-692	E2412	1:500	1 h, RT
1 (2)	F4/80	Bio-Rad	MCA497RT	CI:A3-1	1:200	1 h, RT
2 (1)	CD11c	Cell Signaling	97585	D1V9Y	1:100	1 h, RT
3 (1)	CD4	Cell Signaling	25229	D7D2Z	1:100	4 h, RT
3 (2)	MHC II	eBioscience	14-5321	M5/114.15.2	1:100	4 h, RT
4 (1)	BTK	LS Bio	LS-C180161	Polyclonal	1:200	1 h, RT
4 (2)	CD45	BD Biosci	550539	30-F11	1:50	1 h, RT
5 (1)	PDL1	Cell Signaling	13684	E1L3N	1:50	ON, 4 °C
5 (2)	CD8	eBioscience	14-0808-82	4SM15	1:100	ON, 4 °C
6 (1)	CD3	Thermo	RM-9107-S	SP7	1:300	1 h, RT
6 (2)	CD207	eBioscience	14-2073-82	eBioRMUL.2	1:100	1 h, RT
7 (1)	CD206	Abcam	64693	Polyclonal	1:1000	ON, 4 °C
7 (2)	B220	BD Biosci	550286	R13-6B2	1:100	ON, 4 °C
8 (1)	RORγt	Abcam	207082	EPR20006	1:100	1 h, RT
8 (2)	Foxp3	eBioscience	14-5773-82	FJK16S	1:100	1 h, RT
9 (1)	GATA3	Abcam	199428	EPR16651	1:100	1 h, RT
10 (1)	CD11b	Abcam	133357	EPR1334	1:3000	1 h, RT
11 (1)	TCF1/TCF7	Cell Signaling	2203s	C63D9	1:100	1 h, RT
12 (1)	TIM3	Cell Signaling	83882	D3M9R	1:200	1 h, RT
13 (1)	EOMES	Abcam	183991	EPR19012	1:1000	1 h, RT
14 (1)	Granzyme B	Abcam	4059	Polyclonal	1:200	ON, 4 °C
14 (2)	Ly6G	eBioscience	551459	1A8	1:200	ON, 4 °C
15	Ki67	Abcam	15580	Polyclonal	1:5000	1 h, RT
	Hematoxylin (final)					10 min

ON = overnight; RT = room temperature.

and sections scanned as previously described. Only tissue that survived the entire process was included in the analysis described in the following. The full mIHC protocol, including the order of antibody incubations, is listed in Table 1.

Vascular staining used the previously described process, with just 2 primary antibodies: anti-α smooth muscle actin (1:200, Abcam, ab5694) and anti-CD31 (CD-1, 1:100, LSBio, 4737). Sections were incubated with each primary antibody for 60 minutes at room temperature, and other steps were carried out as previously described.

IMAGE PROCESSING AND ANALYSIS. The image analysis workflow, described previously,[18,19] included 3 main steps: 1) image processing; 2) cell classification; and 3) quantification of cell types. Scanned images were registered in MATLAB version R2018b using the SURF algorithm in the Computer Vision Toolbox (The MathWorks, Inc). Image processing, which included AEC signal extraction and nuclei segmentation, was performed using FIJI (ImageJ)[28]; single cell measurements and cell classification via image gating cytometry were performed in CellProfiler Version 3.5.1[29] and FCS Express 7 Image Cytometry RUO (De Novo Software). Immune cells were classified and quantified using image cytometry in FCS Express based on expression of known discriminatory markers in a gating schema (Table 2). For visualization, signal-extracted images were pseudocolored and overlaid in FIJI. Immune cell lineage values were calculated as a percentage of total $CD45^+$ cells. Subpopulations of leukocytes were calculated as a percentage of the parent population.

For vascular analysis, endothelial cells were defined as $CD31^+$, and smooth muscle cells were defined as α-smooth muscle actin.

ISOLATION AND CULTURE OF PERITONEAL MACROPHAGES. Resident macrophages were harvested from the peritoneum of unoperated C57BL/6J mice. To preserve peritoneal cavity content, the abdominal skin was carefully removed to expose the intact peritoneal wall. Peritoneal lavage was harvested by injecting 10 mL cold 1× PBS into the peritoneal cavity using 20-gauge needles. After brief massaging of the peritoneal wall, the peritoneal lavage was collected using the same needle. Aseptic conditions were maintained throughout the procedure, with special care to avoid microbial contamination via accidental contact with any intestinal or gut tissues. Peritoneal lavage was transferred to a 15 mL

TABLE 2 Multiplex IHC Antibody Panel and Cell Type Identification: Immune Cell Type Identification by Marker Expression

Lineage Identification	All Populations Are CD45$^+$
Th0 (naive) helper T cells	CD3$^+$ CD4$^+$ CD8$^-$ Foxp3$^-$ RORγt$^-$ Tbet$^-$ GATA3$^-$
Regulatory T cells (Tregs)	CD3$^+$CD4$^+$RORγt$^-$FOXP3$^+$GATA3$^-$
Th17 helper T cells	CD3$^+$ CD4$^+$ CD8$^-$ RORγt$^+$
Th2 helper T cells	CD3$^+$CD4$^+$RORγt$^-$FOXP3$^-$GATA3$^+$
CD8$^+$ T lymphocytes (all)	CD3$^+$ CD8$^+$
B cells	CD3$^-$ B220$^+$
Granulocytes	CD3$^-$ B220$^-$ Ly6G$^+$
Macrophages	CD3$^-$ B220$^-$ Ly6G$^-$ F4/80$^+$
Reparative (M2-like) Macrophage	CD3$^-$ B220$^-$ Ly6G$^-$ F4/80$^+$ CSF1R$^+$ CD206$^+$
Inflammatory (M1-like) macrophage	CD3$^-$ B220$^-$ Ly6G$^-$ F4/80$^+$ CSF1R$^+$ CD206$^-$ MHCII$^+$
Inflammatory (M1-like) macrophage	CD3$^-$ B220$^-$ Ly6G$^-$ F4/80$^+$ CSF1R$^+$ CD206$^-$ CD11c$^+$
Dendritic cell	CD3$^-$ B220$^-$ Ly6G$^-$ F4/80$^-$ CD11c$^+$ MHCII$^+$ CD11b$^+$
Interrogation of Functional State of Inflammatory Cells	
Marker	**Classification**
Proliferation	Ki67
Cytotoxicity	Granzyme B
T cell activation	TCF1/TCF7
Identification of Nonimmune Cells	
Cell Type	**Identification (all populations are CD45$^-$)**
Activated fibroblast + SMCs	αSMA$^+$
Endothelial cells	CD31$^+$

conical tube containing 2.0 mL of cell growth media (Dulbecco's Modified Eagle Medium high glucose) and kept on ice. All peritoneal lavages were pooled and centrifuged at 1,500 relative centrifugal force for 5 minutes at 4 °C, and any red blood cells were lysed using red blood cell lysis buffer (Invitrogen, ref. no. 00-4300-54, diluted to 1× in sterile nuclease free water). Peritoneal cells were cultured in DMEM-high glucose containing 10% fetal bovine serum, 1% penicillin-streptavidin, and 5.0 ng/mL colony stimulating factor-1 in normal culture conditions (37 °C, 5% carbon dioxide) for 16 hours. Subsequently, medium was exchanged and cells were treated with 10 μM ISP or 100 nM HJ02 for 24 hours. Additional cells were treated with 100 ng/mL lipopolysaccharide + 5.0 ng/mL interferon-γ) for 6 hours to stimulate differentiation of M1-like macrophages or treated with 10 ng/mL interleukin-4 for 24 hours to stimulate differentiation of M2-like macrophages. At endpoint, medium was discarded, and cells were scraped from plates in 2.0 mL 1× PBS and centrifuged at 1,500 rcf for 5 min at 4 °C. Cell pellets were resuspended in 1.0 mL freezing media (45% DMEM-high glucose, 45% fetal bovine serum, 5% dimethyl sulfoxide) and stored at −80 °C for flow cytometry analysis.

TABLE 3 Antibodies for Flow Cytometry

Target Antigen	Fluorophore	Vendor	Catalog #	Clone	Dilution
MHCII	BV421	BioLegend	107632	M5/114.15.2	1:1000
MHCII	eFluor450	Invitrogen	48-5321-82	M5/114.15.2	1:1000
Ly-6C	BV570	BioLegend	128030	HK1.4	1:200
CD11c	BV605	BioLegend	117334	N418	1:200
CD86	BV650	BioLegend	105035	GL-1	1:200
CD86	BV785	BioLegend	105043	GL-1	1:200
PD-L1	BV711	BD Horizon	563369	M1H5	1:400
F4/80	BV785	BioLegend	123141	BM8	1:150
F4/80	APC	BioLegend	123116	BM8	1:200
CD45	FITC	BioLegend	103108	30-F11	1:600
CD80	PerCP-Cy5.5	BioLegend	104722	16-10A1	1:150
CSF-1R	PE	eBioscience	12-1152-81	AFS98	1:300
CD206	PE-Cy7	BioLegend	141720	C068C2	1:200
CD64	AF647	BioLegend	139322	X54-5/7.1	1:200
CD64	PE-Dazzle594	BioLegend	139320	X54-5/7.1	1:300
CD11b	AF700	BioLegend	101222	M1/70	1:600
CD69	PerCP	BioLegend	104520	H1.2F3	1:200

FLOW CYTOMETRY. Peritoneal macrophages were analyzed using multiparametric flow cytometry. Briefly, frozen samples were thawed and quickly transferred to 1× PBS to dilute the dimethyl sulfoxide in the freezing medium. Single cell suspensions were centrifuged at 1,500 rcf, and cell pellets were stained using Live/Dead Blue (Invitrogen, cat. no. L23105, diluted 1:2500 in 1× PBS) for 10 minutes on ice. Subsequently, cells were treated with Fc Receptor Block (BD Pharmigen, cat. no. 553142, diluted 1:200) for 10 minutes on ice to block nonspecific binding and centrifuged to terminate the Live/Dead staining reaction. Cell pellets were then incubated with fluorescently labeled monoclonal antibodies (Table 3) diluted in a solution of 5% fetal calf serum and 1.0 mM EDTA in 1× PBS (flow buffer). After 30 minutes incubation on ice, cells were washed with flow buffer and fixed with BD CytoFix (BD Bioscience, cat. no. 554655) for 30 minutes on ice. After fixation, cells were washed again and resuspended in flow buffer. Data acquisition was performed on a spectral flow cytometer (Aurora, Cytek). Gating to identify specific immune cell populations was performed using FlowJo software version 10.8 using the gating strategy for identification of macrophages.

STATISTICAL ANALYSIS. Data are presented as mean ± SD. Comparisons among ≥3 groups were analyzed using 1-way analysis of variance (ANOVA), whereas repeated measures ANOVA was used for within-group comparisons. Tukey's or Dunnett's post hoc test for multiple pairwise comparisons was applied to control type I error when comparing all groups or with a control group, respectively. Normality was confirmed with the D'Agostino-Pearson omnibus normality test. Statistical analyses were performed using GraphPad Prism software (version 8 or 9), and a P value <0.05 was considered statistically significant.

FIGURE 2 **ISP, HJ-01 and HJ-02 Injections Promote Sympathetic Reinnervation of the Infarct**

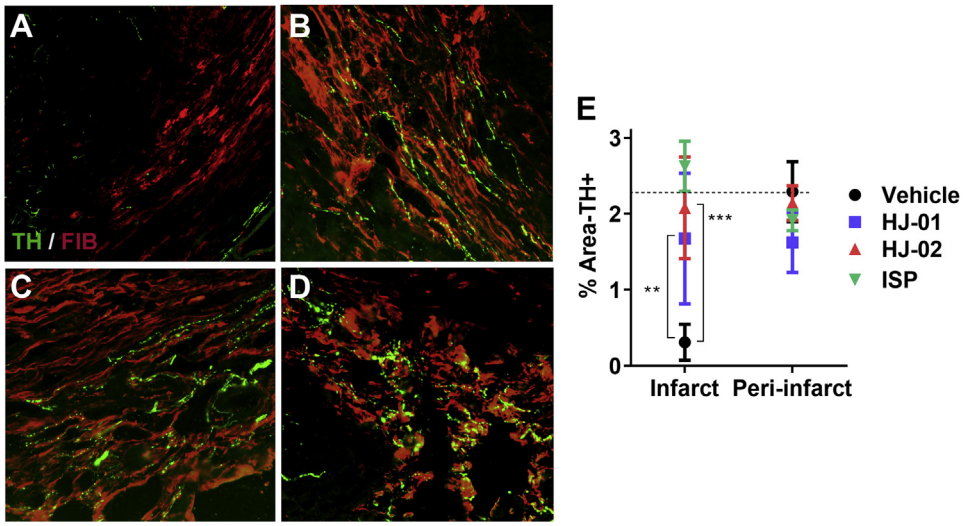

(A-D) Representative images of infarcted left ventricles from mice treated with **(A)** VEH, **(B)** HJ-01, **(C)** HJ-02, and **(D)** ISP 14 days after MI. Sections were stained for tyrosine hydroxylase (TH) to identify sympathetic nerve fibers and fibrinogen to identify the infarct. HJ-01, HJ-02, and ISP treatment resulted in extensive sympathetic reinnervation of the infarct. **(E)** Quantification of TH+ fiber density within the infarct 14 day post-MI (mean ± SD; n = 5/group; $^{**}P < 0.01$; $^{***}P < 0.001$; 2-way ANOVA with Tukey's multiple comparisons post-test). **Dotted line** denotes innervation density in sham animals.

FIGURE 3 **Reinnervation Reduces Arrhythmia Susceptibility After MI**

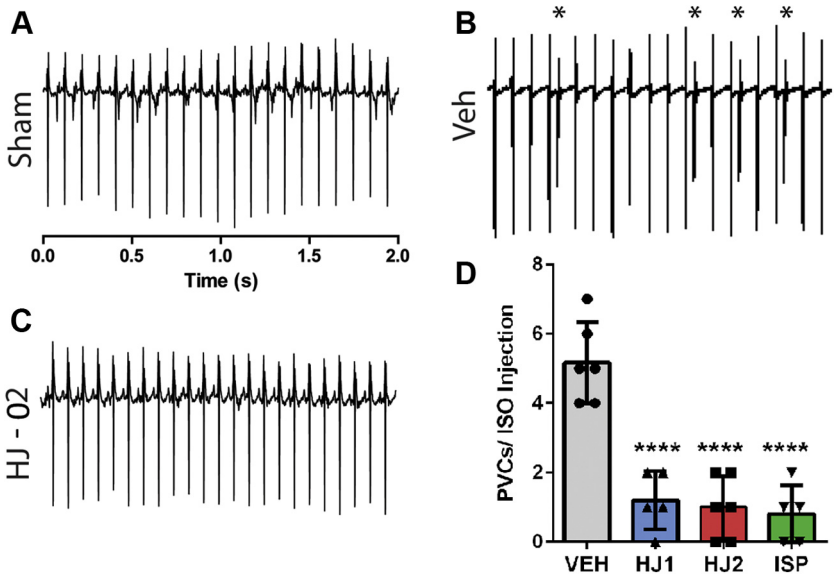

(A to C) Representative electrocardiographic traces recorded in conscious ambulatory animals following **(A)** sham or **(B and C)** MI then treated with either **(B)** VEH or **(C)** HJ-02. Arrhythmias were induced by isoproterenol, and observed premature ventricular complexes (PVCs) are noted with **asterisks**. **(D)** Quantification of arrhythmias during the 45-minute period following isoproterenol injection in all groups. Data are mean ± SD, n = 5/group; $^{***}P < 0.001$; 1-way ANOVA with Dunnett's multiple comparisons post-test. ANOVA = analysis of variance; ISO = isoproterenol; VEH = vehicle.

FIGURE 4 Representative mIHC Staining Used for Immune Cell Quantification

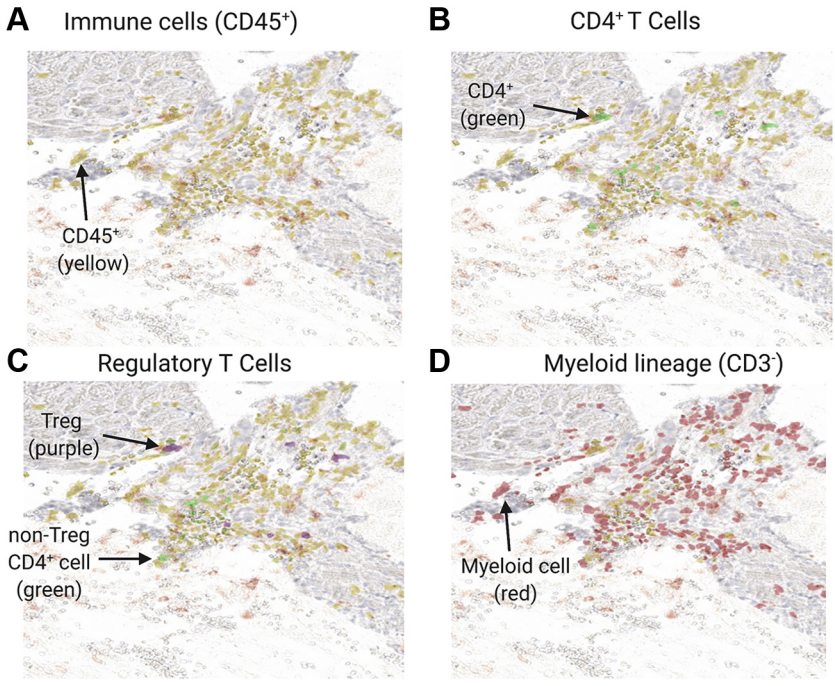

(A) A cardiac section with $CD45^+$ cells shown in **yellow**. To be quantified as an immune cell, cells must have stained positively for CD45. After $CD45^+$ cells were identified, sequential antibody staining was used to phenotype immune cells. $CD4^+$ T cells were identified with $CD3^+$ and $CD4^+$ staining and are shown in **green in B**. Following additional sequential staining, $CD4^+$ cells were further analyzed into subpopulations. T regulatory cells (Tregs) were identified with the cell marker expression of $CD45^+CD3^+CD4^+ROR\gamma T^-FOXP3^+GATA3^-$, and can be seen in **purple in C**. In addition to lymphoid lineage cells, we also detected $CD3^-$ myeloid lineage cells as shown in **red in D**. Notice that none of the cells in the myeloid lineage **(red)** were positive for CD4 (lymphoid lineage). Abbreviation as in Figure 1.

RESULTS

ISP, HJ-01, AND HJ-02 PROMOTE SYMPATHETIC REINNERVATION IN VIVO. We previously established that chondroitin sulfate proteoglycans within the infarct prevent reinnervation despite the presence of nerve growth factor,[9] and that deletion of protein tyrosine phosphatase receptor–σ or disruption of its signaling with ISP restores sympathetic innervation to the infarct.[9,10] ISP modulates the inflammatory response in spinal cord injury,[30] so it was important to use a second therapeutic to identify effects of reinnervation, which should be shared by both treatments. Novel small molecules HJ-01 and HJ-02 promote sympathetic axon outgrowth over chondroitin sulfate proteoglycans in vitro by disrupting protein tyrosine phosphatase receptor-σ–tropomyosin-related kinase A interactions.[20] We first asked whether they stimulated sympathetic regeneration into the cardiac scar 14 days after MI. VEH-treated mice had significant denervation of the infarct on day 14, whereas ISP-, HJ-01–, and HJ-02–treated mice did not. All 3 treatments restored nerve density within the infarct to levels that were not significantly different than the density in sham and the uninjured peri-infarct myocardium (Figure 2).

REINNERVATION PREVENTS ARRHYTHMIAS. Restoring innervation to the infarct with ISP treatment or protein tyrosine phosphatase receptor–σ deletion made hearts less susceptible to arrhythmias.[10] To determine if restoring nerves using HJ-01 and HJ-02 prevented arrhythmias similarly, post-MI mice with electrocardiographic telemetry implants were injected with the β-agonist isoproterenol to mimic circulating catecholamines and provoke arrhythmias. Mice treated with ISP, HJ-01, or HJ-02 to restore nerves had significantly fewer arrhythmias than VEH-treated mice (Figure 3).

TREATMENTS RESTORING SYMPATHETIC INNERVATION ALTER IMMUNE CELL POPULATIONS. Because there was no significant difference in the effect of HJ-01 and HJ-02 on reinnervation and arrhythmias, we moved forward with experiments using only HJ-02. Pilot

FIGURE 5 **Select Immune Cell Populations Are Impacted by Treatments Restoring Innervation**

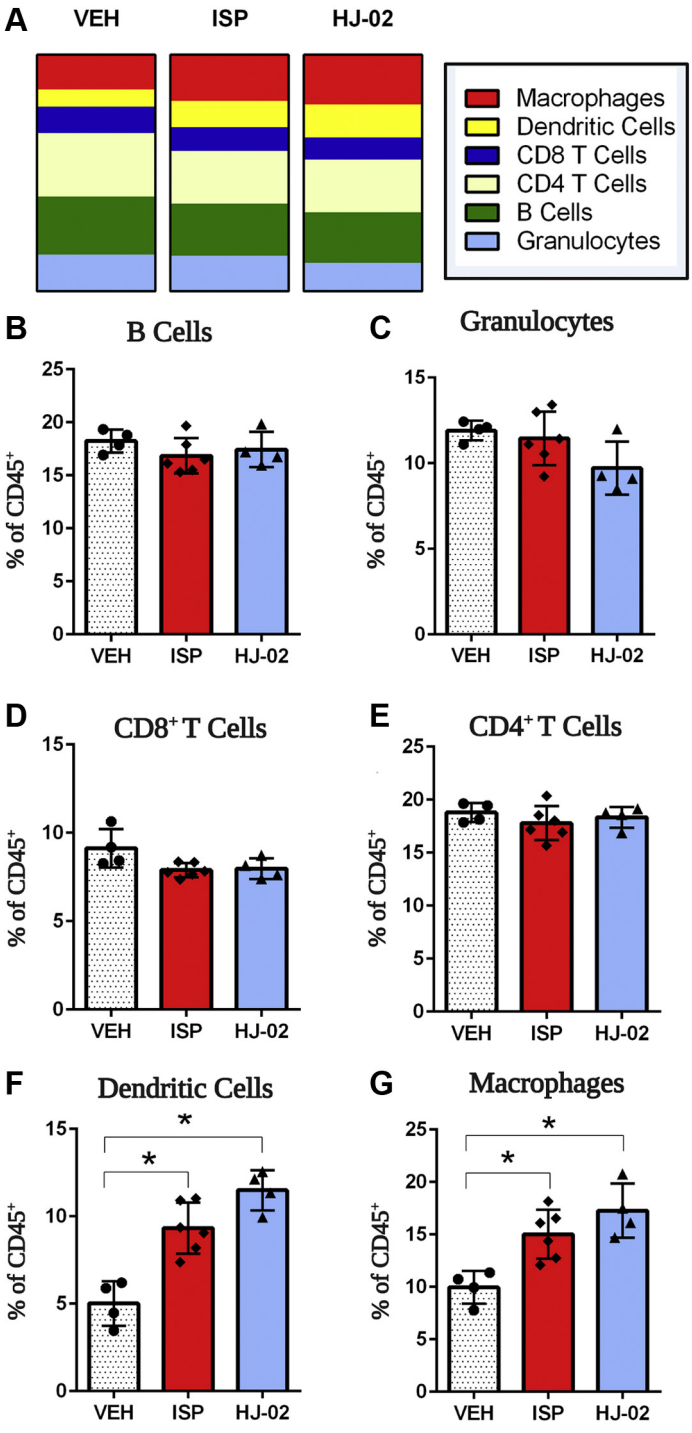

(A) Quantification of immune cell populations from the hearts of mice treated with VEH, ISP, or HJ-02 are shown in **(B to E)**. Quantification of immune cell populations are expressed as a percentage of total CD45+ cells. There was no difference in the percentage of B cells, granulocytes, CD8+ T cells, or CD4+ T cells between any of the groups. **(F)** Hearts from ISP- and HJ-02–treated animals had significantly more dendritic cells compared with VEH. **(G)** Hearts from ISP and HJ-02 treated animals had significantly increased macrophages compared with VEH. Data are mean ± SD, *$P < 0.05$; **$P < 0.01$; ISP, n = 6; VEH and HJ-02, n = 4; 1-way ANOVA with Tukey's multiple comparisons post-test. Abbreviations as in Figures 1 and 3.

FIGURE 6 Macrophage and T Cell Subtypes Are Altered by Treatments Restoring Innervation

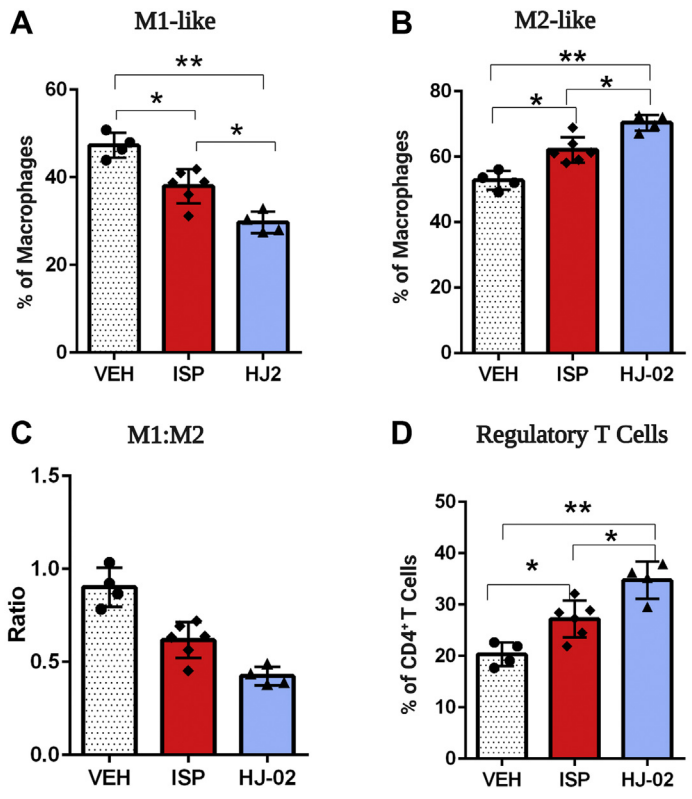

(A and B) Quantification of M1-like and M2-like macrophages, expressed as a percentage of total macrophages. Hearts from ISP- and HJ-02–treated animals had significantly higher levels of M2-like macrophages compared with vehicle (VEH), and hearts from VEH-treated animals had significantly higher levels of M1-like macrophages compared with ISP or HJ-02 treated animals. **(C)** Ratio of M1-like macrophages to M2-like macrophages. **(D)** Quantification of regulatory T cell (Treg) cells, expressed as a percentage of $CD4^+$ T cells. Hearts from ISP- and HJ-02–treated animals had significantly higher levels of Treg cells compared with VEH. Data are mean ± SD. *$P < 0.05$; **$P < 0.01$. ISP (n = 6); VEH and HJ-02 (n = 4); 1-way ANOVA with Tukey's multiple comparisons post-test. Other abbreviations as in Figure 1.

studies of gene expression in the left ventricle comparing VEH- and ISP-treated hearts suggested that sympathetic reinnervation of the developing infarct altered the inflammatory response, with increased expression of growth factors and suppressors of inflammation (Supplemental Figure 2). To test the hypothesis directly, we used mIHC to phenotype leukocytes in the heart 2 weeks after ischemia-reperfusion surgery. Representative mIHC staining used for immune cell quantification is shown in Figures 4A to 4D. The number of B cells, $CD4^+$ T cells, $CD8^+$ T cells, and granulocytes were not different between the ISP and HJ-02 reinnervated hearts and the denervated control hearts (Figures 5B to 5E), but dendritic cells and macrophages were significantly increased in hearts treated with ISP and HJ-02 (Figures 5F and 5G).

TREATMENTS RESTORING SYMPATHETIC INNERVATION SHIFT IMMUNE RESPONSE FROM PRO-INFLAMMATORY TO REPARATIVE PHENOTYPE. Additional differences in the inflammatory response were observed when subtypes of immune cells were identified using multiple lineage selective and phenotypic biomarkers. For example, overall macrophage numbers were increased in reinnervated hearts, but a critical parameter was the relative amount of pro-inflammatory and/or classically activated M1-like macrophages compared to alternatively activated and/or reparative M2-like macrophages. Treatment with either ISP or HJ-02 led to more M2-like reparative and fewer M1-like inflammatory macrophages in the heart after MI. Notably, HJ-02 significantly increased M2 macrophages compared with ISP (Figure 6A) while significantly suppressing M1-like macrophages (Figures 6B and 6C). $CD4^+$ T cells as a group were not affected by reinnervation, but Tregs were significantly increased with ISP or HJ-02 treatment (Figure 6D). Once again, HJ-02 stimulated a significantly larger increase in Treg cells than ISP. Thus, treatments stimulating reinnervation increased the fraction of cells associated with cardiac repair and suppressed cells associated with degradation. HJ-02 treatment generated a significantly greater shift from pro-inflammatory to reparative cell types.

ISP AND HJ-02 DO NOT ALTER THE PHENOTYPE OF PERITONEAL MACROPHAGES. Treating animals with either ISP or HJ-02 restored innervation equally, but HJ-02 generated a greater effect on the inflammatory response. Therefore, we asked if either of these therapeutics had a direct effect on macrophage differentiation in vitro. Peritoneal macrophages were cultured for 24 hours with VEH, ISP (10 μM), or HJ-02 (100 nM) for 24 hours, and then macrophage phenotype was assessed by flow cytometry. Neither ISP nor HJ-02 had any effect on macrophage proliferation or differentiation in vitro (Figures 7B, 7E, and 7F). In contrast, treatment of sister cells with interferon-γ + lipopolysaccharide for 6 hours, or interleukin-4 for 24 hours, stimulated differentiation of M1-like and M2-like macrophages, respectively (Figures 7C to 7F). Although we could not rule out a direct effect of ISP or HJ-02 on macrophage phenotypes in the context of a whole animal, they did not modulate the phenotype of cultured peritoneal macrophages.

HJ-01 AND HJ-02 PREVENT LOSS OF CARDIAC FUNCTION AND REDUCE INFARCT SIZE; ISP DOES NOT. Removal of protein tyrosine phosphatase receptor–σ did not alter infarct size,[10] and we did not expect that treating mice 3 days after reperfusion

FIGURE 7 ISP and HJ-02 Have No Effect on Macrophage Expansion or Polarization

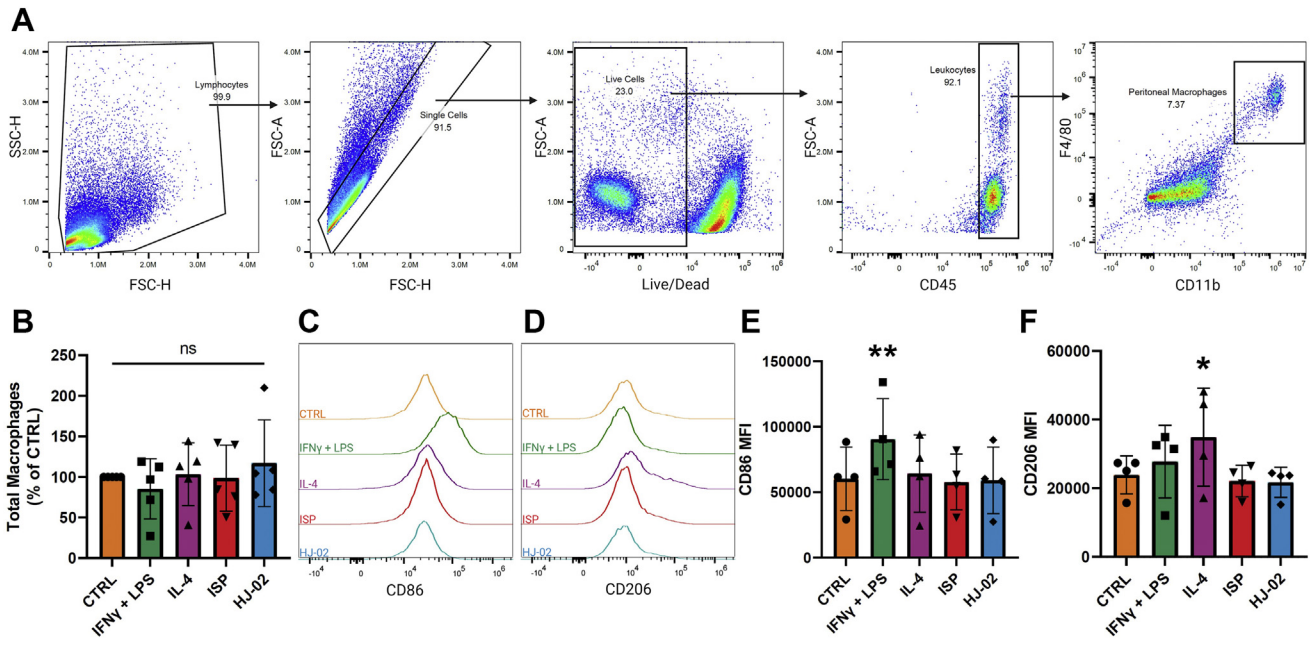

(A) Gating scheme for identifying peritoneal macrophages. **(B)** Quantification of macrophage population levels as a percent of control, normalized to each replicate. Cells were treated with 10 μM ISP or 100 nM HJ02 for 24 hours, and additional cells were treated with 100 ng/mL lipopolysaccharide + 5.0 ng/mL interferon-γ for 6 hours (M1-like) or 10 ng/mL interferon-4 for 24 hours (M2-like). Representative graphs of **(C)** CD86 and **(D)** CD206 expression levels. Graphs of mean fluorescence intensity (MFI) for **(E)** CD86 and **(F)** CD206, quantified via FlowJo v10.8; marker expression in both ISP and HJ-02 treated conditions remains unchanged from control. All data are mean ± SD (n = 4-5 experiments); $*P < 0.05$; $**P < 0.01$ versus control, 1-way ANOVA with Dunnett's multiple comparisons post-test. Abbreviations as in Figure 1.

would have any affect on infarct size. However, the significant shift from pro-inflammatory to reparative macrophages observed following treatment with ISP and HJ-02 led us to ask if infarct size or cardiac function were altered by these treatments or by HJ-01. Cardiac output was measured 15 days after MI, which was 5 days after cessation of treatment. As expected, VEH-treated mice with an MI had significantly reduced ejection fraction and cardiac output compared with sham mice (Figure 8). ISP-treated mice likewise exhibited decreased cardiac output and ejection fraction compared with sham mice. In contrast, mice treated with HJ-01 or HJ-02 exhibited cardiac output and ejection fractions that were similar to sham animals. Infarct size was quantified in the same hearts (Figure 8). Treatment with HJ-01 or HJ-02 beginning 3 days after reperfusion led to significantly smaller infarcts compared with VEH hearts. This was consistent with the improved cardiac function in the HJ-treated hearts and consistent with the greater shift from inflammatory to reparative macrophages in HJ-treated hearts compared with ISP treatment.

HJ-02 DOES NOT ALTER CARDIAC VASCULARIZATION. Microvascular damage is a major contributor to extension of the infarct in the days following ischemia-reperfusion.[31,32] Because we did not treat mice until 3 days after reperfusion, we hypothesized that HJ-02 might be limiting infarct size by protecting the vasculature within the infarct and surrounding tissue, in addition to its effect on the immune system. To quantify the vasculature, we labeled sections for α-smooth muscle actin and CD31 to identify vascular smooth muscle cells and endothelial cells, respectively. We found no difference in the density of vasculature between VEH and HJ-02, regardless of location within the heart (Figure 9). Thus, HJ-02 did not decrease infarct size by promoting revascularization.

DISCUSSION

Proper repair of the myocardium after ischemia-reperfusion requires an orchestrated immune response, with timely activation and suppression of inflammatory mediators to clear necrotic debris and

FIGURE 8 HJ-01 and HJ-02, But Not ISP, Reduce Infarct Size and Preserve Cardiac Function

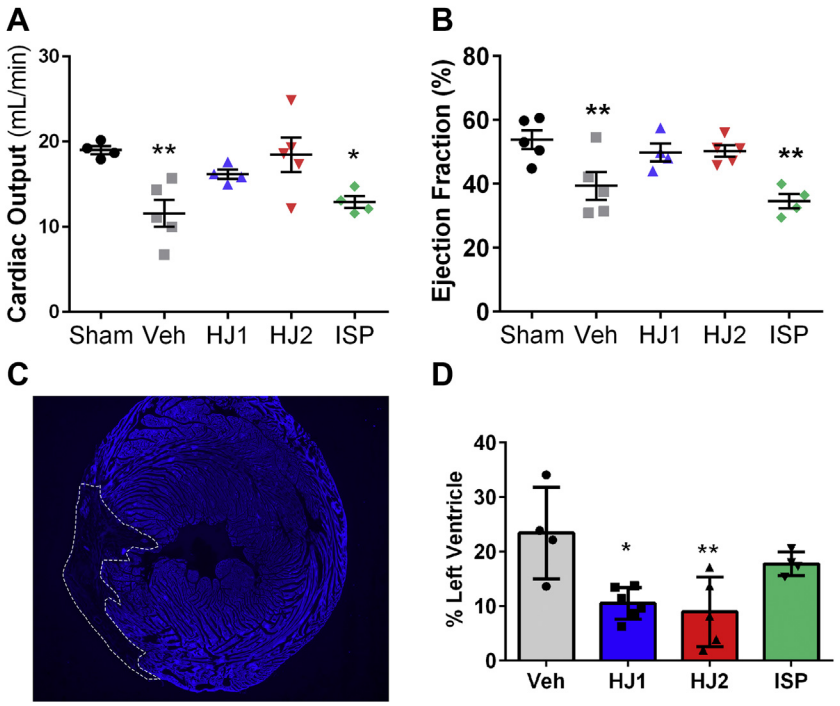

(A and B) Quantification of cardiac output and ejection fraction in mice following sham or myocardial infarction (MI) procedures, then treated with vehicle, HJ-01, or HJ-02. **(C)** Example image of a heart after MI depicting the loss of autofluorescence in the infarct. **(D)** Quantification of infarct size as a percentage of left ventricle in mice treated with HJ-01, HJ-02, or intracellular sigma peptide (ISP). Data are mean ± SD; n = 5/group except sham (n = 4); *$P < 0.05$; **$P < 0.01$; 1-way analysis of variance (ANOVA) with Dunnett's multiple comparisons post-test. (control group = sham mice in **A and B**.

promote tissue repair.[1,2] Despite intense research in this area, there is still much to be elucidated about the types of leukocytes present in the infarcted heart. We applied a novel quantitative mIHC technique in cardiac tissue to provide a more complete perspective of the immune response in the heart following ischemia-reperfusion injury. We quantified immune cells in infarcted hearts, including B cells, $CD4^+$ T cells, $CD8^+$ T cells, dendritic cells, macrophages, and granulocytes. We also identified subpopulations within these larger families, including the traditional M1 pro-inflammatory and M2 reparative phenotypes of macrophages.[33-35] Although recent studies revealed a broader array of macrophage phenotypes under different physiological contexts,[36-41] the M1- and/or M2-like paradigm proved useful in understanding cardiac remodeling and was the nomenclature used in this paper.

Sympathetic noradrenergic transmission modulates immune responses in multiple contexts, having both pro- and anti-inflammatory effects,[15,16] whereas cholinergic transmission is anti-inflammatory in the heart.[17] Cardiac sympathetic nerves release Ach, along with NE, during the first 2 weeks after MI,[14] and we hypothesized that restoring nerves to the cardiac scar would alter the types of immune cells present after MI. However, the nature of those changes was difficult to predict, considering the mixed effects of NE and ACh, and the potential actions of neuropeptide Y, which is also released from cardiac sympathetic nerves. A pilot study that used a quantitative polymerase chain reaction array to quantify left ventricular gene expression suggested that reinnervation stimulated by ISP-enhanced expression of genes associated with suppressing inflammation and stimulating cardiac repair (Supplemental Figure 2). That was confirmed by direct quantification of immune cells using mIHC, which revealed that hearts with reinnervated infarcts exhibited a significantly higher proportion of M2-like reparative macrophages and a lower proportion of M1-like inflammatory macrophages compared with control hearts. Tregs were increased as well, which indicated that the treatments that

FIGURE 9 **HJ-02 and ISP Have No Effect on Vascularization Following MI**

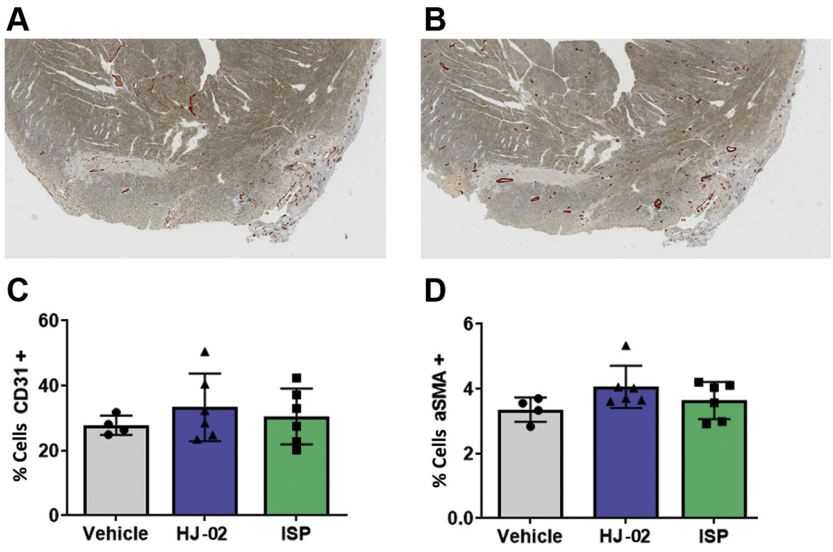

Representative images of an HJ-02–treated mouse heart **(A and B)** stained for CD31 and **(C and D)** α-smooth muscle actin (SMA). Quantification of $CD31^+$ and α-SMA^+ cells in mice treated with VEH, HJ-02, or ISP. Data are mean ± SD n = 4 for vehicle, n = 5-6 for HJ-02 and ISP.

promoted reinnervation of the infarct 5-7 days after ischemia-reperfusion shifted the immune response so that a more reparative phenotype was present 2 weeks after reperfusion.

Despite sympathetic reinnervation in both treatment groups, there were differences in the inflammatory responses that suggested drug-specific effects, in addition to changes caused by reinnervation. This was distinct from the consistent effect of nerve regeneration on decreasing arrhythmia susceptibility. For example, ISP-treated mice had significantly higher proportions of Treg cells and M2-like macrophages than that in VEH-treated mice. However, HJ-02–treated animals had significantly higher numbers of Treg cells and M2-like macrophages compared with ISP animals and control animals. Systemic deletion of protein tyrosine phosphatase receptor–σ had no effect on infarct size,[10] and we did not expect that any treatment that began 3 days after reperfusion in mice would alter infarct size or cardiac output.[42] However, the dramatic shift in immune cells found in the left ventricle 2 weeks after injury suggested that infarct size and cardiac function might be altered in our treated animals. Thus, we quantified cardiac function and infarct size using at least 2 independent observers who were blinded to the treatment groups. HJ-02, which had the greatest effect on the immune response, decreased infarct size and blunted the loss of cardiac function compared with VEH- and ISP-treated animals. The related molecule HJ-01 similarly decreased infarct size and prevented the loss of cardiac output. Neither ISP nor HJ-02 altered the phenotype of cultured peritoneal macrophages, but this does not fully reflect the situation in vivo with multiple additional cell types present, including nerves. Thus, it remains unclear whether drug-specific effects related to ISP prevent it from having a greater impact on inflammation in vivo or whether drug-specific effects of HJ-02 increase its impact on the immune response.

Although it remains unclear if the sympathetic nervous system is solely responsible for the changes we observed in the inflammatory response, NE released from sympathetic neurons could play an important role.[43] NE is present at 10-fold higher concentration than Ach in these neurons,[44] and NE modulates the differentiation and activity of several types of inflammatory cells, including dendritic cells, via β_2AR stimulation.[45-48] Dendritic cells, in turn, alter the activity and differentiation of T cells,[47] and in our study, the proportion of Treg cells was significantly higher in the reinnervated hearts compared with denervated controls. There was also evidence that NE could directly stimulate Treg cells via β_2-ARs.[45] Weirather et al[7] reported that Treg cells enhanced wound healing after MI by promoting differentiation of M2-like macrophages, and that depletion of Treg cells exacerbated myocardial injury.[7] Our data were consistent with these earlier studies and suggested

that restoring sympathetic innervation increased M2 macrophage production via activation of dendritic cells and increased production of Treg cells.

STUDY LIMITATIONS. This study was not without limitations. It was possible that sympathetic reinnervation of the infarcted myocardium had additional effects not observed at the 14-day timepoint of the present study. Adverse cardiac remodeling, such as chamber dilation and the progression of systolic dysfunction to heart failure, did not occur during the 2-week course of the present study. It was possible that reinnervation attenuated pathological remodeling by altering the inflammatory response following MI and slowed or prevented the development of heart failure. Alternatively, restoring NE to the heart might have led to longer term issues with cardiac remodeling that were pathological. Although excess NE in the heart was toxic, we hypothesized that restoring normal noradrenergic transmission during active cardiac remodeling might have long-term beneficial effects. It is an intriguing idea that warrants further research. Despite the expansive list of immune cell markers used in this study, we did not confirm our mIHC results using flow cytometry; follow-up studies will be needed for that. In addition, we did not probe for C-C chemokine receptor 2, and it was possible that our treatments affected the population of C-C chemokine receptor 2 macrophages. Finally, we could not rule out the possibility that our treatments had direct effects on immune cells in vivo, despite their lack of an effect on macrophages in vitro. Culturing macrophages does not reproduce the paracrine signaling from other cell types that may be critical for the change in macrophage phenotype that we observed in vivo.

FUTURE DIRECTIONS. To address these limitations, future research will assess later time points to determine if reinnervation alters the development of heart failure after MI. Additional studies will directly address the role of noradrenergic, cholinergic, and peptidergic transmission in immune modulation, and expand upon our mIHC panel to include additional macrophage markers and cross-validation using flow cytometry. Elucidating the mechanisms that underlie sympathetic modulation of the immune response after MI represents a major emerging opportunity in cardiovascular therapeutics.

CONCLUSIONS

Collectively, our findings indicated that therapeutics ISP and HJ-02 restored sympathetic reinnervation of the infarct and altered the inflammatory response following MI. Reinnervated hearts displayed a smaller proportion of M1-like macrophages than that in control hearts, as well as significantly higher numbers of dendritic cells, M2-like macrophages, and Treg cells compared with control animals. Our present working hypothesis is that drugs that promote sympathetic reinnervation of the infarct increase the proportion and activity of dendritic cells via adrenergic stimulation. These dendritic cells, in turn, increase the number and activity of Treg cells, which go on to promote the differentiation of macrophages into M2-like reparative macrophages.

ACKNOWLEDGMENTS The authors thank Jackie Emathinger, Charlotte Wang, Kimberly Vreugdenhil, and Antoinette Olivas for technical assistance. Paraffin embedding and sectioning was carried out by the OHSU Histopathology Shared Resource. Figure 1 was generated using BioRender.

FUNDING SUPPORT AND AUTHOR DISCLOSURE

This work was supported by the OCTRI Biomedical Innovation Program, the OHSU Bioscience Innovation Program, the M.J. Murdock Charitable Trust and National Institutes of Health grant R01 HL093056. Dr Gardner was supported by the American Heart Association (19POST34460031) and the National Institutes of Health (NIH) (grant T32HL094294). Ms Brooks was supported by NIH (grants UL1GM118964). Dr Sepe was supported by NIH (grant T32HL094294). Dr Habecker was supported by NIH (R01 HL093056). Dr Coussens was supported by NIH (1U01 CA224012, U2C CA233280), the Susan G Komen Foundation, the Knight Cancer Institute, and the Brenden-Colson Center for Pancreatic Care at OHSU. Drs Habecker and Gardner are the co-inventors of technology (ISP) that was used in this research, and that OHSU has licensed to NervGen Pharma Corp. This potential conflict of interest has been reviewed and managed by OHSU. Dr Coussens has been a paid consultant for Cell Signaling Technologies; has received reagent and/or research support from Plexxikon Inc, Pharmacyclics, Inc, Acerta Pharma, LLC, Deciphera Pharmaceuticals, LLC, Genentech, Inc, Roche Glycart AG, Syndax Pharmaceuticals Inc, Innate Pharma, NanoString Technologies, and Cell Signaling Technologies; has been a member of the Scientific Advisory Boards of Syndax Pharmaceuticals, Carisma Therapeutics, Zymeworks, Inc, Verseau Therapeutics, Cytomix Therapeutics, Inc., Kineta Inc, Hibercell, Inc, Cell Signaling Technologies, Alkermes Inc, PDX Pharmaceuticals, Genenta Sciences, and Pio Therapeutics Py Ltd; has been a member of the Lustgarten Therapeutics Advisory working group; and has been a site lead for the AstraZeneca Partner of Choice Network. All other authors have reported that they have no relationships relevant to the contents of this paper to disclose.

ADDRESS FOR CORRESPONDENCE: Dr Beth A. Habecker, Department of Chemical Physiology and Biochemistry, L334, Oregon Health and Science University, 3181 SW Sam Jackson Park Road, Portland, Oregon 97239, USA. E-mail: habecker@ohsu.edu.

PERSPECTIVES

COMPETENCY IN MEDICAL KNOWLEDGE: MI is associated with a robust inflammatory response that plays a crucial role in the repair and remodeling of the infarcted heart. We now understand that initial inflammation and degradation gives way to tissue repair and development of a mature scar. Despite these advances in our understanding of the inflammatory response, development of therapeutics targeting inflammation following MI has been largely unsuccessful. Our data indicate that therapeutics that target the sympathetic nervous system provide a novel approach to shifting the inflammatory response toward a more reparative phenotype, and that this can blunt the loss of cardiac function.

TRANSLATIONAL OUTLOOK: The shift to a reparative immune phenotype with therapeutics that stimulate sympathetic reinnervation of the damaged heart offers a promising target for treatment. The findings merit further mechanistic investigation into sympathetic transmission and its affect on the immune response, including a longer time course following MI to elucidate the potential mitigation of subsequent heart failure. Furthermore, the mIHC method adapted here for use in mouse heart is suitable for characterization of immune cell phenotype in human cardiac biopsies.

REFERENCES

1. Frangogiannis NG. The inflammatory response in myocardial injury, repair, and remodelling. *Nat Rev Cardiol*. 2014;11:255–265.

2. Mouton AJ, Rivera OJ, Lindsey ML. Myocardial infarction remodeling that progresses to heart failure: a signaling misunderstanding. *Am J Physiol Heart Circ Physiol*. 2018;315:H71–H79.

3. Francis Stuart SD, De Jesus NM, Lindsey ML, Ripplinger CM. The crossroads of inflammation, fibrosis, and arrhythmia following myocardial infarction. *J Mol Cell Cardiol*. 2016;91:114–122.

4. Frodermann V, Nahrendorf M. Neutrophil-macrophage cross-talk in acute myocardial infarction. *Eur Heart J*. 2017;38:198–200.

5. Sager HB, Hulsmans M, Lavine KJ, et al. Proliferation and recruitment contribute to myocardial macrophage expansion in chronic heart failure. *Circ Res*. 2016;119:853–864.

6. Bajpai G, Bredemeyer A, Li W, et al. Tissue resident CCR2- and CCR2+ cardiac macrophages differentially orchestrate monocyte recruitment and fate specification following myocardial injury. *Circ Res*. 2019;124:263–278.

7. Weirather J, Hofmann UD, Beyersdorf N, et al. Foxp3+ CD4+ T cells improve healing after myocardial infarction by modulating monocyte/macrophage differentiation. *Circ Res*. 2014;115:55–67.

8. Prabhu SD, Frangogiannis NG. The biological basis for cardiac repair after myocardial infarction: from inflammation to fibrosis. *Circ Res*. 2016;119:91–112.

9. Gardner RT, Habecker BA. Infarct-derived chondroitin sulfate proteoglycans prevent sympathetic reinnervation after cardiac ischemia-reperfusion injury. *J Neurosci*. 2013;33:7175–7183.

10. Gardner RT, Wang L, Lang BT, et al. Targeting protein tyrosine phosphatase sigma after myocardial infarction restores cardiac sympathetic innervation and prevents arrhythmias. *Nat Commun*. 2015;6:6235.

11. Boogers MJ, Borleffs CJ, Henneman MM, et al. Cardiac sympathetic denervation assessed with 123-iodine metaiodobenzylguanidine imaging predicts ventricular arrhythmias in implantable cardioverter-defibrillator patients. *J Am Coll Cardiol*. 2010;55:2769–2777.

12. Fallavollita JA, Heavey BM, Luisi AJ Jr, et al. Regional myocardial sympathetic denervation predicts the risk of sudden cardiac arrest in ischemic cardiomyopathy. *J Am Coll Cardiol*. 2014;63:141–149.

13. Nishisato K, Hashimoto A, Nakata T, et al. Impaired cardiac sympathetic innervation and myocardial perfusion are related to lethal arrhythmia: quantification of cardiac tracers in patients with ICDs. *J Nuclear Med*. 2010;51:1241–1249.

14. Olivas A, Gardner RT, Wang L, Ripplinger CM, Woodward WR, Habecker BA. Myocardial infarction causes transient cholinergic transdifferentiation of cardiac sympathetic nerves via gp130. *J Neurosci*. 2016;36:479–488.

15. Pongratz G, Straub RH. The sympathetic nervous response in inflammation. *Arthritis Res Ther*. 2014;16:504.

16. Körner A, Schlegel M, Kaussen T, et al. Sympathetic nervous system controls resolution of inflammation via regulation of repulsive guidance molecule A. *Nat Commun*. 2019;10:633.

17. Rocha-Resende C, da Silva AM, Prado MAM, Guatimosim S. Protective and anti-inflammatory effects of acetylcholine in the heart. *Am J Physiol Cell Physiol*. 2021;320:C155–C161.

18. Banik G, Betts CB, Liudahl SM, et al. Chapter One: High-dimensional multiplexed immunohistochemical characterization of immune contexture in human cancers. In: Galluzzi L, Rudqvist N-P, eds. *Methods in Enzymology*. Academic Press; 2020:1–20.

19. Tsujikawa T, Kumar S, Borkar RN, et al. Quantitative multiplex immunohistochemistry reveals myeloid-inflamed tumor-immune complexity associated with poor prognosis. *Cell Rep*. 2017;19:203–217.

20. Blake MR, Gardner RT, Jin H, et al. Small molecules targeting PTPsigma-Trk interactions promote sympathetic nerve regeneration. *ACS Chem Neurosci*. 2022;13:688–699.

21. Parrish DC, Alston EN, Rohrer H, et al. Infarction-induced cytokines cause local depletion of tyrosine hydroxylase in cardiac sympathetic nerves. *Exp Physiol*. 2010;95:304–314.

22. Dobaczewski M, Bujak M, Zymek P, Ren G, Entman ML, Frangogiannis NG. Extracellular matrix remodeling in canine and mouse myocardial infarcts. *Cell Tissue Res*. 2006;324:475–488.

23. Ma Y, Iyer RP, Jung M, Czubryt MP, Lindsey ML. Cardiac fibroblast activation post-myocardial infarction: current knowledge gaps. *Trends Pharmacol Sci*. 2017;38:448–458.

24. McCarroll CS, He W, Foote K, et al. Runx1 deficiency protects against adverse cardiac remodeling after myocardial infarction. *Circulation*. 2018;137:57–70.

25. Lang BT, Cregg JM, DePaul MA, et al. Modulation of the proteoglycan receptor PTPsigma promotes recovery after spinal cord injury. *Nature*. 2015;518:404–408.

26. Parrish DC, Francis Stuart SD, Olivas A, et al. Transient denervation of viable myocardium after myocardial infarction does not alter arrhythmia susceptibility. *Am J Physiol Heart Circ Physiol*. 2018;314:H415–H423.

27. Lorentz CU, Parrish DC, Alston EN, et al. Sympathetic denervation of peri-infarct

myocardium requires the p75 neurotrophin receptor. *Exp Neurol*. 2013;249:111–119.

28. Schindelin J, Arganda-Carreras I, Frise E, et al. Fiji: an open-source platform for biological-image analysis. *Nat Methods*. 2012;9:676–682.

29. Carpenter AE, Jones TR, Lamprecht MR, et al. CellProfiler: image analysis software for identifying and quantifying cell phenotypes. *Genome Biol*. 2006;7:R100.

30. Dyck S, Kataria H, Alizadeh A, et al. Perturbing chondroitin sulfate proteoglycan signaling through LAR and PTPsigma receptors promotes a beneficial inflammatory response following spinal cord injury. *J Neuroinflamm*. 2018;15:90.

31. Bekkers SC, Smulders MW, Passos VL, et al. Clinical implications of microvascular obstruction and intramyocardial haemorrhage in acute myocardial infarction using cardiovascular magnetic resonance imaging. *Eur Radiol*. 2010;20:2572–2578.

32. Siao CJ, Lorentz CU, Kermani P, et al. ProNGF, a cytokine induced after myocardial infarction in humans, targets pericytes to promote microvascular damage and activation. *J Exp Med*. 2012;209:2291–2305.

33. Buscher K, Ehinger E, Gupta P, et al. Natural variation of macrophage activation as disease-relevant phenotype predictive of inflammation and cancer survival. *Nat Commun*. 2017;8:16041.

34. Mills CD, Kincaid K, Alt JM, Heilman MJ, Hill AM. M-1/M-2 macrophages and the Th1/Th2 paradigm. *J Immunol*. 2000;164:6166–6173.

35. Zhu L, Zhao Q, Yang T, Ding W, Zhao Y. Cellular metabolism and macrophage functional polarization. *Int Rev Immunol*. 2015;34:82–100.

36. Ginhoux F, Guilliams M, Merad M. Expanding dendritic cell nomenclature in the single-cell era. *Nat Rev Immunol*. 2022;22:67–68.

37. Guilliams M, Ginhoux F, Jakubzick C, et al. Dendritic cells, monocytes and macrophages: a unified nomenclature based on ontogeny. *Nat Rev Immunol*. 2014;14:571–578.

38. Murray PJ, Allen JE, Biswas SK, et al. Macrophage activation and polarization: nomenclature and experimental guidelines. *Immunity*. 2014;41:14–20.

39. Ruffell B, Coussens LM. Macrophages and therapeutic resistance in cancer. *Cancer Cell*. 2015;27:462–472.

40. Ma Y, Mouton AJ, Lindsey ML. Cardiac macrophage biology in the steady-state heart, the aging heart, and following myocardial infarction. *Transl Res*. 2018;191:15–28.

41. Nahrendorf M, Swirski FK. Abandoning M1/M2 for a network model of macrophage function. *Circ Res*. 2016;119:414–417.

42. Bulluck H, Yellon DM, Hausenloy DJ. Reducing myocardial infarct size: challenges and future opportunities. *Heart*. 2016;102:341–348.

43. Sanders VM, Straub RH. Norepinephrine, the beta-adrenergic receptor, and immunity. *Brain Behav Immun*. 2002;16:290–332.

44. Wang L, Olivas A, Francis Stuart SD, et al. Cardiac sympathetic nerve transdifferentiation reduces action potential heterogeneity after myocardial infarction. *Am J Physiol Heart Circ Physiol*. 2020;318:H558–H565.

45. Guereschi MG, Araujo LP, Maricato JT, et al. Beta2-adrenergic receptor signaling in CD4+ Foxp3+ regulatory T cells enhances their suppressive function in a PKA-dependent manner. *Eur J Immunol*. 2013;43:1001–1012.

46. Nijhuis LE, Olivier BJ, Dhawan S, et al. Adrenergic β2 receptor activation stimulates anti-inflammatory properties of dendritic cells in vitro. *PLoS One*. 2014;9:e85086.

47. Takenaka MC, Araujo LP, Maricato JT, et al. Norepinephrine controls effector T cell differentiation through β2-adrenergic receptor-mediated inhibition of NF-κB and AP-1 in dendritic cells. *J Immunol*. 2016;196:637–644.

48. Turner MD, Nedjai B, Hurst T, Pennington DJ. Cytokines and chemokines: at the crossroads of cell signalling and inflammatory disease. *Biochim Biophys Acta*. 2014;1843:2563–2582.

KEY WORDS inflammation, macrophages, multiplex IHC, myocardial infarction, sympathetic nervous system

APPENDIX For expanded Methods and Results as well as supplemental figures, please see the online version of this paper.